ORGANIC PROCESS RESEARCH & DEVELOPMENT
OPR&D
Article
Cite This: Org. Process Res. Dev. 2019, 23, 2707−2715
pubs.acs.org/OPRD

Scale-Up of the Manufacturing Process To Produce Docetaxel-Loaded mPEG-*b*-p(HPMA-Bz) Block Copolymer Micelles for Pharmaceutical Applications

Jaleesa Bresseleers,[†,‡] Mahsa Bagheri,[§] Gert Storm,[§,∥] Josbert M. Metselaar,[⊥] Wim E. Hennink,[§] Silvie A. Meeuwissen,[†] and Jan C. M. van Hest*[,‡]

[†]ChemConnection BV - Ardena Oss, 5349 AB Oss, The Netherlands
[‡]Department of Bio-Organic chemistry, Eindhoven University of Technology, 5600 MB Eindhoven, The Netherlands
[§]Department of Pharmaceutics, Utrecht Institute for Pharmaceutical Sciences (UIPS), Faculty of Science, Utrecht University, 3508 TB Utrecht, The Netherlands
[∥]Section - Targeted Therapeutics, Department of Biomaterials Science and Technology, Faculty of Science and Technology, University of Twente, 7522 NB Enschede, The Netherlands
[⊥]Department of Nanomedicine and Theranostics, Institute for Experimental Molecular Imaging RWTH University Clinic, 52074 Aachen, Germany

Supporting Information

ABSTRACT: An efficient, scalable, and good manufacturing practice (GMP) compatible process was developed for the production of docetaxel-loaded poly(ethylene glycol)-*b*-poly(*N*-2-benzoyloxypropyl methacrylamide) (mPEG-*b*-p(HPMA-Bz)) micelles. First, the synthesis of the mPEG-*b*-p(HPMA-Bz) block copolymer was optimized through step-by-step investigation of the batch synthesis procedures. This resulted in the production of 1 kg of mPEG-*b*-p(HPMA-Bz) block copolymer with a 5 kDa PEG block and an overall molecular weight of 22.5 kDa. Second, the reproducibility and scalability of micelle formation was investigated for both batch and continuous flow setups by assessing critical process parameters. This resulted in the development of a new and highly efficient continuous flow process, which led to the production of 100 mL of unloaded micelles with a size of 55 nm. Finally, the loading of the micelles with the anticancer drug docetaxel was successfully fine-tuned to obtain precise control on the loaded micelle characteristics. As a result, 100 mL of docetaxel-loaded micelles (20 mg/mL polymer and 5 mg/mL docetaxel in the feed) with a size of 55 nm, an encapsulation efficiency of 65%, a loading capacity of 14%, and stable for at least 2 months in water at room temperature were produced with the newly developed continuous flow process. In conclusion, this study paves the way for efficient and robust large-scale production of docetaxel-loaded micelles with high encapsulation efficiencies and stability, which is crucial for their applicability as a clinically relevant drug delivery platform.

KEYWORDS: *polymeric micelles, nanomedicines, continuous flow, docetaxel, scalability, block copolymer*

INTRODUCTION

Long-standing developments in the field of nanomedicine have resulted in a range of promising nanocarrier formulations for drug delivery.[1−4] For example, polymeric micelles, which are core−shell nanoparticulate structures composed of amphiphilic polymers, have attracted much attention. Their hydrophobic core allows for the accommodation and potentially improved pharmacokinetics of poorly water-soluble drugs such as quite some chemotherapeutics used for cancer treatment. The hydrophilic shell of polymer micelles, often based on the hydrophilic poly(ethylene glycol) (PEG), provides colloidal stability and stealth-like properties.[5−10]

Despite promising preclinical results and their high pharmaceutical and economical potential,[2,11] there are still some important hurdles that typically appear in the development process of nanomedicines. A main challenge that needs to be tackled is the scalable and reproducible production of not only the building blocks but also the drug-loaded assembled nanoparticles. This challenge is even more prominent in the relatively new area of nanomedicine due to the complexity of the chemistry required (since nanoparticles are usually assemblies of multiple components), the manufacturing process, and the quality control, which should all match with the standards of GMP.[12−14] Besides that, the instability of the nanoparticles is also a typical issue that needs attention. During early experimentation and preclinical research programs, these crucial aspects are often not studied. This is reflected by very limited publications regarding scalability, reproducibility, and process development toward GMP production of nanomedicines.

Recently, a highly promising polymer micelle formulation based on poly(ethylene glycol)-*block*-poly(*N*-2-benzoyloxypropyl methacrylamide) (mPEG-*b*-p(HPMA-Bz)) was reported.[15−17] These micelles demonstrated high drug loading for paclitaxel and docetaxel (DTX), drug retention, and particle stability as a result of the $\pi-\pi$ stacking and hydrophobic interactions enabled by the hydrophobic benzyl

Received: September 9, 2019
Published: October 29, 2019

DOI: 10.1021/acs.oprd.9b00387
Org. Process Res. Dev. 2019, 23, 2707−2715

groups containing blocks in the core of the micelles. In this contribution, the chemotherapeutic drug DTX was chosen as a model drug for the loading of the micelles since it is a clinically well-established drug that presents high therapeutic efficacy against a range of solid tumors. In general, the application of DTX is limited by its dose-dependent neurotoxic side effects and its high hydrophobic nature. For the latter, solubility enhancers such as Cremophor EL are used, which in turn are associated with hypersensitivity reactions.[18] In previous studies, it was shown that DTX can be encapsulated with high efficiency because of its high hydrophobicity and the presence of aromatic groups in its molecular structure contributing to the $\pi-\pi$ stacking interactions in the core of the mPEG-*b*-p(HPMA-Bz) micelles.[15]

The goal of the research described in this contribution was to develop an efficient, scalable, and highly controlled process for the manufacturing of the newly developed DTX-loaded polymer micelles based on mPEG-*b*-p(HPMA-Bz), keeping GMP regulations in mind. This was achieved by first optimizing the four-step synthesis of the mPEG-*b*-p(HPMA-Bz) building block with a fixed molecular weight of the mPEG of 5 kDa and an aimed molecular weight of the p(HPMA-Bz) block between 15−20 kDa. Subsequently, a thorough evaluation of batch production versus continuous flow processes was performed to enable the selection of the preferred preparation methodology for both unloaded and drug-loaded micelles at a large scale.

MATERIALS AND METHODS

Materials. DL-1-amino-2-propanol, methacryloyl chloride, sodium hydroxide (NaOH), sodium chloride (NaCl), magnesium sulfate ($MgSO_4$), benzoyl chloride, triethyl amine (TEA), benzoic anhydride, 4,4′-azobis(4-cyanopentanoic acid) (ABCPA), *N*,*N*′-dicyclohexylcarbodiimide (DCC), and trichloroacetyl isocyanate (TAIC) were obtained from Sigma-Aldrich (Darmstadt, Germany) and used without further purification. Poly(ethylene glycol) methyl ether (mPEG) (5 kDa) was obtained from Polysciences (Warrington, USA) and dried in a vacuum stove overnight at 70 °C. Docetaxel was obtained from Alfa Aesar (Kandel, Germany) and used without further purification. All solvents were purchased from commercial suppliers and used as received.

Monomer Synthesis. *N-(2-Hydroxypropyl) methacrylamide (HPMA).* HPMA was synthesized through the reaction between DL-1-amino-2-propanol and methacryloyl chloride (Scheme 1) without adding more stabilizing antioxidant. The

Scheme 1. Synthesis of HPMA

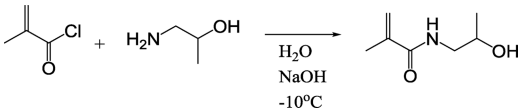

synthesis was performed by mixing 1 equiv of DL-1-amino-2-propanol (1066 mL, 13.78 mol) with 1.2 equiv of NaOH (1475 mL of 11.2 M NaOH) and 1500 mL water. This solution was stirred and brought to −10 °C. Then, 1.05 equiv of methacryloyl chloride (1400 mL, 14.46 mol, containing ∼200 ppm monomethyl ether hydroquinone as stabilizer) was added dropwise in 90−120 min, while allowing the temperature to rise to 10 °C in the first 30 min. Thereafter, the temperature was kept constant at 10 °C. After the addition of all the methacryloyl chloride, the temperature was allowed to reach room temperature and the reaction was stirred for another 30 min. The mixture was analyzed using thin layer chromatography (TLC; SiO_2, eluent: toluene/acetone 6/4, coloring agent: $KMnO_4$ stain) to verify complete conversion of the reaction. Once the reaction was completed, three liquid extractions with 1500 mL of toluene each were performed to remove apolar byproducts. The product was then isolated by a liquid extraction with 3 L of dichloromethane (DCM). Then, five more liquid extractions, each using 1500 mL of a DCM/methanol (9:1) mixture, were performed. Each extract was analyzed using TLC. The combined product layers were dried with $MgSO_4$ and filtered, and the product was obtained after solvent evaporation in vacuo at 30 °C. The product was recrystallized in acetone (100 g of product in approximately 100 mL of hot solvent) followed by slowly cooling down the solution to room temperature and then storing overnight at 2−7 °C. The HPMA crystals were collected through filtration, dried under vacuum to remove remaining acetone, and analyzed by ^{1}H-NMR and HPLC.

N-(2-Benzoyloxypropyl) methacrylamide (HPMA-Bz). HPMA-Bz was synthesized through the coupling reaction of HPMA and benzoyl chloride, (no stabilizer was added) and using triethyl amine (TEA) as a base (Scheme 2). One

Scheme 2. Synthesis of HPMA-Bz

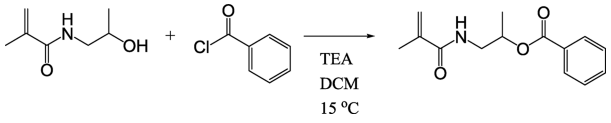

equivalent of HPMA (1041 g, 7.27 mol) and 1.43 equiv of TEA (1457 mL, 10.4 mol) were dissolved in 1 L of DCM. Once all the HPMA was dissolved, the homogeneous solution was cooled to 15 °C. Then, 1.43 equiv of benzoyl chloride (1207 mL, 10.4 mol) was added dropwise, while keeping the temperature at 15 °C. After complete addition of benzoyl chloride, the mixture was allowed to reach room temperature and stirred overnight. The solution was filtered to remove the formed TEA HCl salt, and unreacted HPMA was removed through extraction with 1 L of water three times. The product-containing DCM layer was dried with MgSO4, filtered, and evaporated in vacuo. The obtained powder was stirred in 2 L of heptane to remove benzoic anhydride. Both benzoic anhydride and benzoic acid are present in trace amounts in the benzoyl chloride starting material, but both are also formed by reaction of benzoyl chloride with water to benzoic acid and as was shown by Dhimitruka et al. in the presence of TEA will eventually lead to the formation of benzoic anhydride.[19] The heptane was removed by filtration, and the solid−liquid extraction cycle was repeated until all the benzoic anhydride was removed, as detected by HPLC (in general after two extractions). The product was dried in vacuo at 30 °C and analyzed via HPLC and ^{1}H-NMR.

Macroinitiator (MI) Synthesis. The mPEG-ABCPA-mPEG macroinitiator (MI) was synthesized, as previously described,[20] through an esterification of 1 equiv ABCPA and 2 equiv of mPEG (Scheme 3). For this synthesis, 3 equiv of DCC was used as a coupling reagent, and 0.3 equiv of 4-(dimethylamino)pyridinium 4-toluenesulfonate (DPTS) was used as a catalyst (Scheme 3). ABCPA, mPEG, and DPTS (12 g of ABCPA, 450 g of mPEG, and 4 g of DPTS) were dissolved

DOI: 10.1021/acs.oprd.9b00387
Org. Process Res. Dev. 2019, 23, 2707−2715

Scheme 3. Synthesis of mPEG-ABCPA-mPEG Macroinitiator

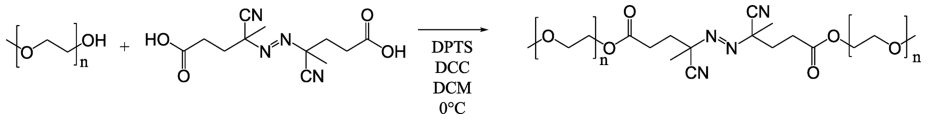

Scheme 4. Synthesis of mPEG-*b*-p(HPMA-Bz)

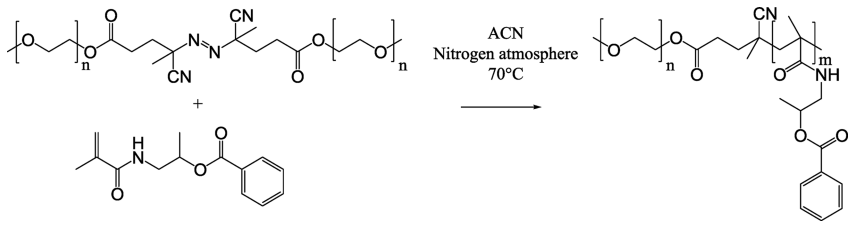

in 2.25 L of DCM, and the solution was brought to 0 °C and under a nitrogen atmosphere. Then, 26 g of DCC was dissolved in 2.25 L of DCM and added dropwise to the cooled solution. This mixture was left to react overnight at room temperature and subsequently filtered to remove precipitated 1,3-dicyclohexylurea (DCU). The product was precipitated in cold methyl-*tert*-butylether (MTBE), collected through filtration, and dried in vacuo. The product was then analyzed by GPC and ^{1}H-NMR.

Polymerization. mPEG-*block*-poly(*N*-2-benzoyloxypropyl methacrylamide) (mPEG-*b*-p(HPMA-Bz)) block copolymer was synthesized via free radical polymerization using mPEG-ABCPA-mPEG as macroinitiator (MI) and *N*-(2-benzoyloxypropyl methacrylamide) (HPMA-Bz) as monomer, as was described earlier (Scheme 4).[15−17] The MI and monomer were dissolved in ACN at a total concentration of 300 g/L with a molar feed ratio of MI/HPMA-Bz (1:200 mol/mol). More specifically, 1367 g of HPMA-Bz and 300 g of MI were dissolved in 5.5 L of ACN, and the polymerization was conducted at 70 °C under a nitrogen atmosphere for 24 h. The resulting mPEG-*b*-p(HPMA-Bz) block copolymer was collected through precipitation in cold MTBE (1 L of product in ACN to 5 L of MTBE) followed by filtration. To remove the unreacted monomer from the product, the polymer powder was dissolved in ACN (300 g/L) and reprecipitated in cold MTBE (1 L of product in ACN to 5 L of MTBE). After filtration and drying of the product in vacuo, the polymer was analyzed by ^{1}H-NMR and GPC.

Poly(*N*-2-benzoyloxypropyl methacrylamide) p(HPMA-Bz) homopolymer was synthesized using the same procedure, via free radical polymerization using ABCPA as initiator and HPMA-Bz as monomer. They were dissolved in ACN at a total concentration of 0.3 g/ mL with a molar feed ratio of ABCPA/HPMA-Bz (1:200 mol/mol). More specifically, 3 g of HPMA-Bz and 0.017 g of ABPCA were dissolved in 10 mL of ACN, and the polymerization was conducted at 70 °C under a nitrogen atmosphere for 24 h. Workup was exactly the same as described for the mPEG-*b*-p(HPMA-Bz) block copolymer.

Homopolymer Removal. The polymerization procedure of the mPEG-*b*-p(HPMA-Bz) block copolymer, as described in the previous section, might result also in the formation of p(HPMA-Bz) homopolymer. As pointed out and demonstrated in our previous paper, this homopolymer will solubilize in the core of the micelles, leading to an increase in micelle size.[20] To maintain a highly controllable and reproducible process for the production of micelles with a size of 50−60 nm, a procedure was developed to remove the p(HPMA-Bz) homopolymer from the polymer mixture.

mPEG-*b*-p(HPMA-Bz) spiked with 10% p(HPMA-Bz) was dissolved in ethanol (2 g in 20 mL). Since the polymers did not dissolve in ethanol at ambient temperature, the mixture was heated to 70 °C. This heated solution was then rapidly added to room temperature water in a 1:1 volume ratio while continuously stirring. The precipitate was removed by centrifugation (15 min, 2886 g), and both the supernatant and the precipitate were dried in a vacuum oven at 40 °C overnight to obtain the purified mPEG-*b*-p(HPMA-Bz) from the supernatant. Both the product and the precipitate (homopolymer) were analyzed using GPC and ^{1}H-NMR.

The described procedure above was also employed for the synthesized block copolymer to ensure no presence of homopolymer.

Micelle Preparation in Batch. mPEG-*b*-p(HPMA-Bz) micelles were prepared in batch by dissolving the homopolymer-free mPEG-*b*-p(HPMA-Bz) in THF (20 mg/mL) and pipetting 1 mL into 1 mL of Milli-Q water as nonsolvent. After THF evaporation overnight, this nanoprecipitation method results in the formation of micelles. Prior to analysis, the micelle dispersions were filtered through a 0.2 μm disk filter. Residual THF content was determined using GC-headspace. The size of the micelles was determined by dynamic light scattering (DLS).

Instead of THF evaporation overnight, THF can also be removed by placing the 2 mL polymer/THF/Milli-Q mixture in a regenerated cellulose dialysis bag with a cutoff at 12−14 kDa and dialyzing against Milli-Q water overnight.

Micelle Preparation in Continuous Flow. mPEG-*b*-p(HPMA-Bz) micelles were prepared in continuous flow by dissolving the homopolymer-free mPEG-*b*-p(HPMA-Bz) block copolymer in THF (20 mg/mL). A homemade setup consisting of two piston pumps was used, both at 1 mL/min, to pump both the polymer/THF mixture and Milli-Q water via different inlets through a T-mixer to ensure rapid mixing (Figure 1). The outlet stream was collected in a flask and continuously stirred until a total of 200 mL was collected. The THF was removed through tangential flow filtration (TFF) and replaced by Milli-Q water using a Sius-LS TFF Hystream, MWCO 100 kDa, 0.02 m^2 cassette. Due to the low compatibility of the membrane with THF, the micelle dispersion was diluted 10 times using Milli-Q water prior to loading onto the membrane. Next, using the TFF setup, the micelle dispersion was concentrated to 20 mg/mL and the

DOI: 10.1021/acs.oprd.9b00387
Org. Process Res. Dev. 2019, 23, 2707−2715

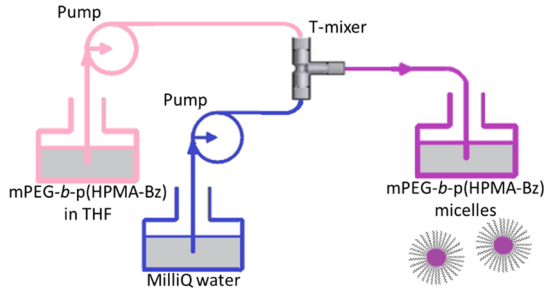

Figure 1. Schematic representation of the continuous flow setup.

concentrated dispersion was further purified with four diafiltration volumes of water to ensure complete THF depletion. Eventually, this process resulted in the production of 100 mL of micellar dispersion with a concentration of 20 mg of polymer/mL Milli-Q. Residual THF content was determined using GC headspace. The size of the micelles was determined by dynamic light scattering (DLS).

Preparation of Docetaxel-Loaded Micelles. DTX-loaded mPEG-*b*-p(HPMA-Bz) micelles were prepared using the same procedures as for the unloaded micelles described above, both in batch and in flow. DTX was codissolved with the polymer in THF (20 mg of polymer and 5 mg of DTX/mL THF). Using the batch setup, 1 mL of the polymer/DTX in THF was pipetted to 1 mL of Milli-Q water. THF was removed by either evaporation overnight or overnight dialysis against Milli-Q water using a regenerated cellulose dialysis bag with a cutoff at 12−14 kDa. Using the continuous flow setup, two piston pumps were used, both at 1 mL/min, to pump the polymer/DTX in THF mixture and Milli-Q water through a T-mixer to ensure rapid mixing. The outlet stream was collected in a flask and continuously stirred until a total of 200 mL was collected. The THF was removed through TFF, as described above, resulting in the production of 100 mL of micellar dispersion with a concentration of 20 mg of polymer/mL Milli-Q. The dispersion was first filtered through a 0.45 μm disk filter and then through a 0.2 μm disk filter to remove free DTX. The latter filtration step can also be used for sterilization purposes. The size of the DTX-loaded micelles was measured by DLS, and the encapsulation efficiency of DTX in the micelles was determined by HPLC. Residual THF content was determined using GC-headspace.

Stability Study. The stability of the unloaded and DTX-loaded micelles was determined by storing samples at 4 °C and at room temperature for a period up to 2 months. At different time points, samples of the stored micelle dispersions were filtered through a 0.2 μm disk filter to remove released/free DTX. The size of the DTX-loaded micelles was measured by DLS, and the remaining DTX in the micelles was determined by HPLC.

^{1}H-NMR. Approximately 20 mg of the product was dissolved in 700 μL (for HPMA, HPMA-Bz, mPEG-b-p(HPMA-Bz) and p(HPMA-Bz), DMSO-d6 was used as the solvent and for the MI, $CDCl_3$ was used as the solvent) and measured using a 400 MHz NMR with a 5 mm PABBO BB probe from Bruker.

The amount of unreacted mPEG-OH in the MI product was determined by TAIC. Five drops of TAIC were added to the NMR tube and after 20 min, a ^{1}H-NMR spectrum was recorded. Using TAIC, the signal of the methylene group neighboring the terminal hydroxyl group was reported to shift from 4.2 to 4.4 ppm.[21] The amount of unreacted mPEG-OH was subsequently determined based on the peak areas.[17,22] The M_n of the block copolymer, before and after removal of the homopolymer, as well as the M_n of the removed homopolymer, were determined using the following formula

$$M_n = (\text{integral at 8.0 ppm}/2 \times \text{molecular weight of HPMA} - \text{Bz}) + 5000\ \text{g/mol}$$

Content ^{1}H-NMR. Content ^{1}H-NMR can be used to give information on the content or percentage of total compound present in an obtained product. This is done by adding a known amount of an internal standard with a distinct integration area compared to those of the tested compound. In our case for HPMA-Bz, approximately 20 mg of HPMA-Bz was dissolved in 700 μL DMSO-d6 and measured using a 400 MHz NMR with a 5 mm PABBO BB probe from Bruker. For determination of the content, ∼9 mg of maleic acid was added to the samples as an internal reference content standard (99.94%). The content of the compound can be calculated using the following formula

$$P_x = \frac{I_x \times N_{std} \times M_x \times W_{std}}{I_{std} \times N_x \times M_{std} \times W_x} \times P_{std} = \frac{0.94 \times 2 \times 247.29\ \text{g/mol} \times 9.62\ \text{g}}{2 \times 1 \times 116.07\ \text{g/mol} \times 19.55\ \text{g}} \times 99.94\% = 98.55\%$$

where P_x is the content of the sample (% m/m), P_{std} is the content of the standard (% m/m), I_x is one of the integration areas of the HPMA-Bz sample (in our case the one at 5.59 ppm), I_{std} is the integration area of the standard at 6.28 ppm, N_x is the number of protons (1 proton) of the integrated peak at 5.59 ppm of the HPMA-Bz sample, N_{std} is the number of protons (2 protons) of the integrated peak of the standard, M_x is the molecular weight of the sample (247.29 g/mol), M_{std} is the molecular weight of the standard (116.07 g/mol), W_x is the weight of the sample (mg), and W_{std} is the weight of the standard (mg).

HPLC. The synthesized HPMA and HPMA-Bz, and the encapsulated DTX were analyzed via high-performance liquid chromatography (HPLC) by injecting 1 μL, using an Agilent XDB-C18 (50 × 4.6 mm, 1.8 μm) column and a gradient flow of 1 mL/min, going from 95% of 0.1% formic acid in water and 5% of 0.05% formic acid in acetonitrile (ACN) to 95% of 0.05% formic acid in ACN and 5% of 0.1% formic acid in water. Detection was done at 254 nm for HPMA and HPMA-Bz and at 230 nm for DTX. HPMA and HPMA-Bz samples were prepared by dissolving 20 mg in 1 mL of ACN. For the determination of DTX loading, samples were prepared by dissolving 50 μL of filtered micelle dispersion in 950 μL of ACN. This mixture was vortexed to ensure complete disassembly of the micelles and a homogeneous distribution of DTX in the solution.

The remaining ABCPA in de MI product was analyzed and quantified via HPLC by injecting 10 μL, using an XBridge C8 (50 × 4.6 mm, 5 μm) column and a gradient flow of 1 mL/min, going from 98% of 0.1% formic acid in water and 5% of 0.05% formic acid in acetonitrile (ACN) to 95% of 0.05% formic acid in ACN and 5% of 0.1% formic acid in water. Detection was done at 210 nm. Samples were prepared by dissolving 20 mg of MI in 1 mL of ACN.

DOI: 10.1021/acs.oprd.9b00387
Org. Process Res. Dev. 2019, 23, 2707−2715

GPC. The MI and the synthesized mPEG-*b*-p(HPMA-Bz) before and after homopolymer removal were analyzed by GPC to measure the number-average molecular weight (M_n), weight-average molecular weight (M_w), and molecular weight distribution using a PSS PFG analytical linear S column and PEGs of narrow molecular weights as calibration standards. The samples were prepared by dissolving approximately 5 mg in 1 mL of DMF containing 10 mM LiCl. Samples of 20 μL were injected and eluted with DMF containing 10 mM LiCl as the eluent. The elution rate was 0.7 mL/min, with a temperature of 40 °C, and the sample was detected using a refractive index detector.

Gas Chromatography Headspace Analysis (GC-Headspace). To determine residual solvent in the micellar dispersions, GC-headspace was conducted. A Shimadzu GC-2010 equipped with a flame ionization detector and Shimadzu HS-20 headspace autosampler was used together with a 30 m × 0.32 mm capillary column with a film thickness of 0.25 μm. For the internal standard, a stock solution was prepared by dissolving 150 μL of 2-propanol (analytical standard) in water using a volumetric 100 mL flask. One milliliter of this solution was transferred into another 100 mL volumetric flask and diluted to the 100 mL volume with DMF. The standard, used for the calibration, was made by pipetting 300 μL analytical grade THF in a 50 mL volumetric flask, which was diluted to volume with DMF. One milliliter of this stock was transferred to a 100 mL volumetric flask and diluted to volume with DMF to get a THF concentration of 1067 ppm. One milliliter of this standard solution was mixed with 4 mL of internal standard stock solution and put in a 20 mL GC-headspace vial. The samples were prepared dissolving 50 μL of micellar dispersion in 1 mL of DMF. To this mixture, 4 mL of internal standard stock solution was added, and the mixture was put in a 20 mL GC-headspace vial. The flow rate of nitrogen was 1.8 mL/min. All measurements were done in triplicate.

DLS. For dynamic light scattering (DLS) measurements, a Malvern Zetasizer nano series ZS90 with a measurement angle of 173° and a temperature of 25 °C was used. Concentrations were approximately 20 mg/mL, without further diluting after production.

Cryogenic Transmission Electron Microscopy (Cryo-TEM) Analysis. Cryo-TEM measurements were performed on loaded and unloaded, batch made, and in flow made micelles. The samples were prepared on Quantifoil R 2/2 grids. In short, 3 μL of micellar dispersion was pipetted onto a grid and blotted for 3 s using a fully automated vitrification robot (MARK III) at 20 °C and 100% relative humidity. The grid was then rapidly plunged and frozen in liquid ethane. Micrographs were taken using an FEI Tecnai G2 Sphera (200 kV electron source) equipped with LaB6 filament utilizing a cryoholder or an FEI Titan (300 kV electron source) equipped with an autoloader station.

RESULTS AND DISCUSSION

To attain a clinically applicable nanomedicine formulation, all aspects of the production, from monomer synthesis to preparation of the drug-loaded particles, have to be done in a commercially feasible and reproducible manner. Synthesis was therefore performed on a kilogram scale. Furthermore, in the preclinical preparation protocol, a number of adjustments had to be made to achieve this level of scalability. In the following sections, the different steps are discussed in detail.

Monomer Synthesis. *HPMA Synthesis.* In a publication of Kopeček and Bažilová, HPMA was synthesized by reaction of methacryloyl chloride with 1-amino-2-propanol in acetonitrile at 0 °C.[23] We later switched to a Schotten−Baumann reaction overnight where 1-amino-2-propanol was stirred in a two-layer system of water and DCM while NaOH was titrated together with the methacryloyl chloride to neutralize the formed HCl, resulting in a ∼80% yield.[15−17]

In the present study, however, a new method was developed in which it was decided to perform the reaction in water only with an excess of NaOH. The presence of this excess neutralizes the formed HCl. An additional advantage of this method was that the reaction was completed in less than 3 h instead of overnight. Additionally, after purification and workup, this reaction resulted in an excellent yield of ∼90% and 99.9% purity according to HPLC (Figures S1 and S2).

HPMA-Bz Synthesis. HPMA-Bz was synthesized by the reaction of HPMA and benzoyl chloride. The latter contained trace amounts of benzoyl anhydride, as detected by HPLC (Figure S3). During the HPMA-Bz synthesis, it was shown that even more benzoyl anhydride was formed, probably due to the reaction of benzoyl chloride with water present in the used DCM (Figure S5). This anhydride remained present during regular workup procedures, and therefore, an adequate extraction method was developed to remove this impurity from the solid HPMA-Bz. Multiple solvents were tested for a solid−liquid extraction process, including acetone, ACN, ethanol, methanol, and heptane. It was found that heptane was able to dissolve and extract the remaining anhydride from the product because HPMA-Bz is essentially insoluble in this solvent. After a solid−liquid extraction, followed by filtration and drying of the powder, HPMA-Bz was obtained in a yield of ∼85% and a purity of 99.3%, as determined by HPLC (Figure S6) and a content of 98.5% as determined by content ^{1}H-NMR (Figure S7).

Macroinitiator Synthesis. Following a recently optimized procedure,[20] the mPEG-ABCPA-mPEG MI ($mPEG_{5K}$) was successfully synthesized on a large scale (450 g). The only difference with the previous method was that the product was precipitated in MTBE and collected through filtration instead of centrifugation. The total yield of the synthesized MI was very high (∼97%).

As described in the Materials and Methods section, there is a possibility that the monofunctionalized initiator mPEG-ABCPA is formed upon MI synthesis, leading to the formation of unwanted p(HPMA-Bz) homopolymer during radical polymerization. This homopolymer will be solubilized in the core of the micelles, which in turn will result in an increase in micellar size.[20] Analysis of the synthesized MI by GPC showed that approximately 9% impurity was present in the form of a molecular species with 5 kDa molecular weight, which corresponds to the monofunctionalized initiator mPEG-ABCPA and /or free mPEG (Figure S9). Analysis by ^{1}H-NMR using TAIC, which allowed to detect the free OH group of unreacted PEG, showed that the impurity of the MI with free mPEG-OH also amounted to 9%, indicating that the product only contained a trace amount of mPEG-ABCPA (Figure S10). It was envisioned that using this MI would result in only very low amounts of the homopolymer p(HPMA-Bz). However, there is also a possibility that nonfunctionalized ABCPA is present in the mixture, which will give p(HPMA-Bz) upon polymerization. The detection limit of ABCPA together with MI was determined to be 0.1 wt %. Further HPLC

DOI: 10.1021/acs.oprd.9b00387
Org. Process Res. Dev. 2019, 23, 2707−2715

analysis was not able to detect any ABCPA in the actual MI mixture and therefore indicated that only very low amounts of ABCPA were present (below 0.1 wt %), if present at all (Figure S13). The total yield of the synthesized MI was very high (~97%).

Polymerization of HPMA-Bz Using mPEG-ABCPA-mPEG as Macroinitiator. The mPEG-*b*-p(HPMA-Bz) block copolymer was successfully synthesized on a scale of ~1.6 kg, using mPEG-ABCPA-mPEG as macroinitiator. After two precipitations in cold MTBE, mPEG-*b*-p(HPMA-Bz) was obtained with a yield of ~71% with only trace amounts of residual monomer, as determined by ^{1}H-NMR (Figure S17).

Even though the formation of p(HPMA-Bz) homopolymer was reduced, due to the optimization of the procedure of the mPEG-ABCPA-mPEG macroinitiator, some homopolymer is still present in the mixture, which probably comes from nonfunctionalized ABCPA present in the mixture. Therefore, a method was successfully developed to remove even trace amounts of p(HPMA-Bz) homopolymer. This newly developed method can be found in the Materials and Methods section. Upon performing this method, ~15% of precipitation was removed from the block copolymer mixture. It was shown by ^{1}H-NMR that the precipitate in ethanol has a weight fraction of mPEG present of only 2% (Figure S18). This is 10 times smaller than envisioned for normally synthesized block copolymer and would give a block copolymer with an M_n of 222.3 kDa. This indicates that it was indeed mainly p(HPMA-Bz) homopolymer that precipitated. With the homopolymer removed, approximately 1 kg of the purified mPEG-*b*-p(HPMA-Bz) block copolymer (M_n, 22.5 kDa) was eventually obtained.

This mPEG-*b*-p(HPMA-Bz) block copolymer product did not contain detectable residual monomer, as detected by ^{1}H-NMR, and the molecular weights were determined by ^{1}H-NMR (M_n, 22.5 kDa) and GPC (M_n, 19.3 kDa and M_w, 21.6 kDa). (Figures S16 and S19).

Micelle Preparation. In previous studies, the micelles were prepared through a nanoprecipitation method.[16,20] Purified mPEG-*b*-p(HPMA-Bz) was dissolved in THF and pipetted into water. This solution was left overnight in a fume hood for THF to spontaneously evaporate. For obvious reasons, when working on a large scale with multiple liters of solution, this is not a feasible method. An attempt was therefore made to remove the THF in vacuo, which unfortunately resulted in aggregation and visual precipitation of the polymeric material. As a result, it was decided to remove THF using dialysis. A simple dialysis was performed for the polymer THF/water solution against water in a dialysis bag with a cutoff at 12−14 kDa. This resulted in the formation of micelles with an average diameter of ~57 nm and a narrow size distribution (PDI) lower than 0.1 according to DLS. This was in agreement with the solvent evaporation method that yielded a size of ~55 nm and a PDI < 0.1. To replace the batch-wise dialysis process into a scalable procedure, continuous transient flow filtration (TFF) was explored.

Previous research showed that if supersaturation upon mixing is not obtained, micelle formation will result in poorly defined micelles of varying sizes.[20] To reduce the risk in these variations and therefore ensure supersaturation of the mixture, the polymer was dissolved at high concentration (20 mg/mL) in THF, and the ratio in which this solution was added to water was kept at 1:1 while collecting the micelle dispersions under continuous stirring. This was first tested on a small scale, collecting only 10 mL and evaporating the THF overnight in a fume hood, which resulted in the formation of micelles with a mean size of 55 nm and a PDI lower than 0.1. With the continuous flow preparation, larger amounts of micellar dispersions were prepared, diluted, concentrated, and purified by TFF. This resulted in the production of 100 mL of micellar dispersion in water with a concentration of 20 mg of polymer/mL and a residual THF content below the detection limit of GC-headspace and therefore conform safety regulations. The mean size of the micelles was 55 nm and the PDI was below 0.1, which is the same as the micelles produced using the batch setup. The produced micelle dispersion was split in two parts, which were stored at 4 °C and at room temperature. After 2 months, no precipitation or changes in size and PDI were observed for both storage conditions. It is envisioned that even up to multiple liters can be prepared using this newly developed continuous flow method.

Preparation of Docetaxel-Loaded Micelles. For the preparation of DTX-loaded mPEG-*b*-p(HPMA-Bz) micelles, mPEG-*b*-p(HPMA-Bz) was dissolved in THF (20 mg/mL), and subsequently, DTX was added and dissolved (final concentration was 5 mg/mL). The preparation method was first tested on a small scale in a fume hood. To this end, 1 mL of the polymer/DTX solution was added to 1 mL of water, and the THF was removed either by evaporation overnight in the fume hood or by dialysis against water. Both methods resulted in the formation of micelles with a mean size of 55 nm and PDI below 0.1, which is a similar size and PDI as the nonloaded micelles. Cryo-TEM imaging showed no difference between the structures of the loaded versus the nonloaded micelles (Figure 2). HPLC analysis showed that the

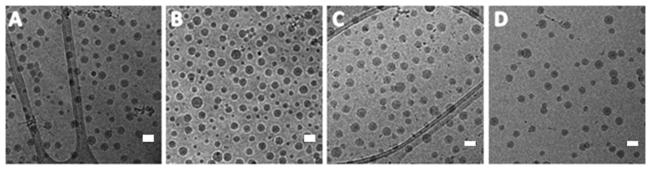

Figure 2. Cryo-TEM images of the mPEG-*b*-p(HPMA-Bz) micelles. Scale bars correspond to 50 nm. (A) Unloaded and prepared in batch (average diameter, 29 nm). (B) DTX-loaded and prepared in batch (average diameter, 28 nm). (C) Unloaded and prepared using continuous flow (average diameter, 28 nm). (D) DTX-loaded and prepared using continuous flow (average diameter, 27 nm).

encapsulation efficiency was ~85% for the evaporated samples and ~65% for the dialyzed samples (Figure 3). The loading capacities were determined to be ~17.5 and ~14% respectively.

One possible hypothesis for this difference in encapsulation efficiencies relies on the difference between the two workup methods that leads to a difference in the final concentration of DTX in the dispersions. During dialysis, THF is passively replaced by water and therefore the micelle dispersion is diluted, whereas during evaporation, THF is removed leaving a more concentrated dispersion. It is hypothesized that not all DTX is perfectly partitioned into the micellar cores with part of it located into the PEG corona. Once the micelle dispersion is then diluted during dialysis, the DTX that is present in the corona area will be released rapidly. In that case, visible precipitation of DTX is observed. For the micelles prepared using the evaporation method, this is not the case. It is envisioned that over time, the DTX that is present in the

DOI: 10.1021/acs.oprd.9b00387
Org. Process Res. Dev. 2019, 23, 2707−2715

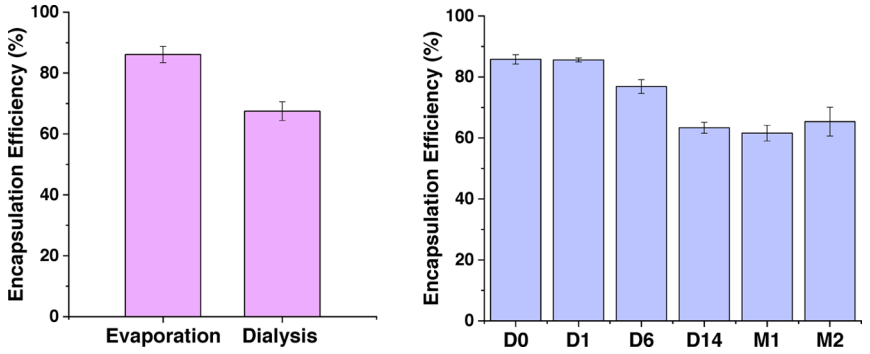

Figure 3. Encapsulation efficiencies of DTX-loaded micelles using batch mode (left) and the evaporation and dialysis methods for workup and the results of a stability study (right) at room temperature of the DTX-loaded micelles that were prepared using the solvent evaporation method. Time points are day 0 (D0), after 1 day (D1), after 6 days (D6), after 2 weeks (D14), after 1 month (M1), after 2 months (M2).

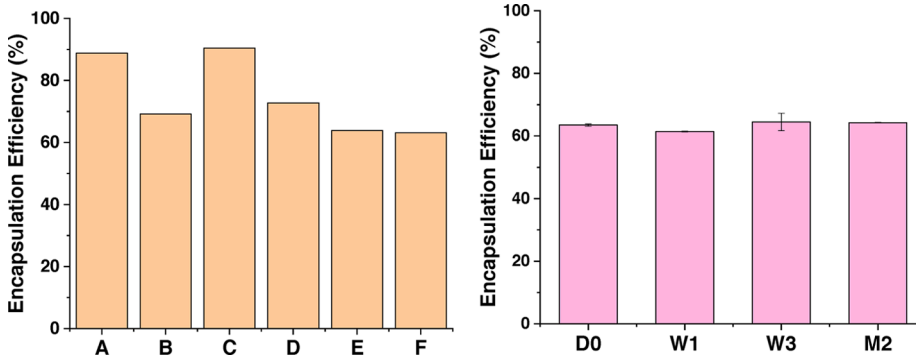

Figure 4. Encapsulation efficiencies of DTX (left) of the different steps and controls during DTX-loaded micelle production using a continuous flow process. (A) After overnight evaporation of THF; (B) After dialysis against water; (C) After filtration over a 0.2 μm disk filter and overnight evaporation; (D) After diluting 10 times; (E) After concentrating to a 20 mg/mL polymer; (F) Final DTX-loaded micelle product. (right) Stability study at room temperature of the DTX-loaded micelles that were produced in continuous flow. Time points are starting point (D0), after 1 week (W1), after 3 weeks (W3), and after 2 months (M2).

corona area will be slowly released. Eventually, only DTX that is partitioned in the micelle cores will remain in the micelle dispersion and will be retained for a prolonged period of time.

The stability of the DTX-loaded micelles that were prepared using the solvent evaporation method was followed upon incubation of the micellar dispersions at room temperature for 2 months. The micellar size distribution remained similar over this entire period, whereas the encapsulation efficiency decreased from ~85 to ~65% in 2 weeks. This latter value resembles the DTX-loaded micelles that were produced using the dialysis method. On the contrary, looking into the stability of the DTX-loaded micelles produced in batch mode using dialysis, the encapsulation efficiency did not decrease over time (Figure S20). This reinforces the hypothesis that not all DTX is partitioned in the micellar core and that a part is located in the PEG corona. For the dialysis workup, as mentioned before, no decrease in encapsulation efficiency was observed over time since all the DTX that was absorbed into the corona was already released due to the dilution factor. For the evaporation workup, this is not the case and the DTX that is located in the PEG corona will be released over time in the stability study. This result demonstrates that for reproducible micelle preparation, a dialysis method is preferred.

DTX-loaded micelles were also prepared using the newly developed continuous flow procedure. The DTX/polymer in THF solution was continuously added to Milli-Q water at a 1:1 flow ratio with a total flow rate of 2 mL/min, using two piston pumps, until a total volume of 200 mL was obtained. Out of this dispersion, two 1 mL samples were taken: for one, THF was removed by overnight evaporation (Figure 4A) and the other sample was dialyzed against water (Figure 4B). The remaining ~200 mL micelle dispersion was filtered over a 0.2 μm disk filter. A 1 mL sample was taken after filtration, and THF was removed by overnight evaporation (Figure 4C). The micelle dispersion was then diluted 10 times (Figure 4D) and, by using TFF, concentrated to a 20 mg polymer/mL (Figure 4E). As a final purification step, the micelle dispersion was washed with four diafiltration volumes, thus four times with 100 mL of Milli-Q water to obtain the final DTX-loaded micelle product (Figure 4F) without any detectable residual THF as measured by GC-headspace. Analysis of the intermediate steps and the final product confirmed similar behavior regarding encapsulation efficiency as was observed for the small-scale productions. Once the micelle dispersion was further diluted with water, either by dialysis or simple addition of the water, the encapsulation efficiency dropped from approximately 85 to 65%. Micelle size distributions did remain constant with an average size of 55 nm and a PDI below 0.1, identical to those sizes obtained for the small-scale production methods. Cryo-TEM imaging confirmed these results (Figure 2).

The stability of the DTX-loaded micelles regarding drug retention, made using the continuous flow setup, was followed for a period of 2 months. After 2 months, the micelle size distribution and encapsulation efficiency did not change significantly (Figure 4 and Figure S19). This reinforces the

DOI: 10.1021/acs.oprd.9b00387
Org. Process Res. Dev. 2019, 23, 2707−2715

hypothesis that upon micelle formation, not all DTX is solubilized in the micellar core and that a part is present at the core−shell interface or even in the more hydrophilic mPEG corona. Most noteworthy, very stable particles with negligible DTX release during storage were produced on a large scale. The described continuous flow production process can be likely translated into a large-scale manufacturing process for the production of liters of loaded micelles suitable for clinical evaluation.

CONCLUSIONS

The goal of this study was to develop an efficient, scalable, and highly controlled process for the manufacturing of DTX-containing nanoparticles based on polymer micelles assembled from the amphiphilic block copolymer mPEG-*b*-p(HPMA-Bz). The results demonstrate an excellent and optimized process for the large batch synthesis on ∼1 kg scale of mPEG-*b*-p(HPMA-Bz) ($mPEG_{5K}$, M_n 22.5 kDa). It is important to know that the amount of polymer produced is sufficient for the production of enough micelle formulation to go through the first phase of clinical trials. Using this polymer, micelles were easily made by both batch and continuous flow setups. Comparison of the results and feasibility for larger scale production indicates a clear preference to use the continuous flow setup. Since the most important parameters for homogenous micelle formation are mixing and saturation conditions, polymer micelles were efficiently made in a reproducible manner regarding particle size using a continuous flow processing. The loading of mPEG-*b*-p(HPMA-Bz) with DTX was very efficient, with outstanding encapsulation efficiency of ∼65% and a loading capacity of 14%. Moreover, the drug-loaded micelles retained the encapsulated drug over a prolonged period of time. Most importantly, the production methodology described herein to produce the loaded nanoparticles can be readily translated for production under GMP conditions for future clinical trials.

ASSOCIATED CONTENT

Supporting Information

The Supporting Information is available free of charge on the ACS Publications website at DOI: 10.1021/acs.oprd.9b00387.

HPLC chromatograms, ^{1}H-NMR spectra, GPC chromatograms, encapsulation efficiencies, and DLS data (PDF)

AUTHOR INFORMATION

Corresponding Author

*E-mail: J.C.M.v.Hest@tue.nl.

ORCID

Wim E. Hennink: 0000-0002-5750-714X

Jan C. M. van Hest: 0000-0001-7973-2404

Notes

The authors declare no competing financial interest.

ACKNOWLEDGMENTS

The authors are grateful for financial support received from the European Union's Horizon 2020 research and innovation program Marie Sklodowska-Curie Innovative Training Networks (ITN) under grant no. 676137.

REFERENCES

(1) van Elk, M.; Murphy, B. P.; Eufrásio-da-Silva, T.; O'Reilly, D. P.; Vermonden, T.; Hennink, W. E.; Duffy, G. P.; Ruiz-Hernández, E. Nanomedicines for advanced cancer treatments: Transitioning towards responsive systems. *Int. J. Pharm.* **2016**, *515*, 132−164.

(2) Hare, J. I.; Lammers, T.; Ashford, M. B.; Puri, S.; Storm, G.; Barry, S. T. Challenges and strategies in anti-cancer nanomedicine development: An industry perspective. *Adv. Drug Delivery Rev.* **2017**, *108*, 25−38.

(3) Duncan, R.; Vicent, M. J. Polymer therapeutics-prospects for 21st century: The end of the beginning. *Adv. Drug Delivery Rev.* **2013**, *65*, 60−70.

(4) Björnmalm, M.; Thurecht, K. J.; Michael, M.; Scott, A. M.; Caruso, F. Bridging bio-nano science and cancer nanomedicine. *ACS Nano* **2017**, *11*, 9594−9613.

(5) Mikhail, A. S.; Allen, C. Block copolymer micelles for delivery of cancer therapy: Transport at the whole body, tissue and cellular levels. *J. Controlled Release* **2009**, *138*, 214−223.

(6) Houdaihed, L.; Evans, J. C.; Allen, C. Overcoming the road blocks: advancement of block copolymer micelles for cancer therapy in the clinic. *Mol. Pharmaceutics* **2017**, *14*, 2503−2517.

(7) Deng, C.; Jiang, Y.; Cheng, R.; Meng, F.; Zhong, Z. Biodegradable polymeric micelles for targeted and controlled anticancer drug delivery: Promises, progress and prospects. *Nano Today* **2012**, *7*, 467−480.

(8) Varela-Moreira, A.; Shi, Y.; Fens, M. H. A. M.; Lammers, T.; Hennink, W. E.; Schiffelers, M. Clinical application of polymeric micelles for the treatment of cancer. *Mater. Chem. Front.* **2017**, *1*, 1485−1501.

(9) Cagel, M.; Tesan, F. C.; Bernabeu, E.; Salgueiro, M. J.; Zubillaga, M. B.; Moretton, M. A.; Chiappetta, D. A. Polymeric mixed micelles as nanomedicines: Achievements and perspectives. *Eur. J. Pharm. Biopharm.* **2017**, *113*, 211−228.

(10) Cabral, H.; Kataoka, K. Progress of drug-loaded polymeric micelles into clinical studies. *J. Controlled Release* **2014**, *190*, 465−476.

(11) Sainz, V.; Conniot, J.; Matos, A. I.; Peres, C.; Zupančič, E.; Moura, L.; Silva, L. C.; Florindo, H. F.; Gaspar, R. S. Regulatory aspects on nanomedicines. *Biochem. Biophys. Res. Commun.* **2015**, *468*, 504−510.

(12) Shi, J.; Kantoff, P. W.; Wooster, R.; Farokhzad, O. C. Cancer nanomedicine: progress, challenges and opportunities. *Nat. Rev. Cancer* **2016**, *17*, 20.

(13) Hua, S.; de Matos, M. B. C.; Metselaar, J. M.; Storm, G. Current trends and challenges in the clinical translation of nanoparticulate nanomedicines: Pathways for translational development and commercialization. *Front. Pharmacol.* **2018**, *9*, , DOI: 10.3389/fphar.2018.00790.

(14) Tinkov, S. Chapter 15 - Contemporary industrial practice for manufacturing of nanomedicines. *Emerging Applications of Nanoparticles and Architecture Nanostructures* Elsevier Inc.: 2018.

(15) Shi, Y.; van Steenbergen, M. J.; Teunissen, E. A.; Novo, L.; Gradmann, S.; Baldus, M.; van Nostrum, C. F.; Hennink, W. E. Π-Π Stacking increases the stability and loading capacity of thermosensitive polymeric micelles for chemotherapeutic drugs. *Biomacromolecules* **2013**, *14*, 1826−1837.

(16) Shi, Y.; van der Meel, R.; Theek, B.; Oude Blenke, E.; Pieters, E. H. E.; Fens, M. H. A. M.; Ehling, J.; Schiffelers, R. M.; Storm, G.; van Nostrum, C. F.; Lammers, T.; Hennink, W. E. Complete regression of xenograft tumors upon targeted delivery of paclitaxel via Π-Π stacking stabilized polymeric micelles. *ACS Nano* **2015**, *9*, 3740−3752.

(17) Naksuriya, O.; Shi, Y.; van Nostrum, C. F.; Anuchapreeda, S.; Hennink, W. E.; Okonogi, S. HPMA-based polymeric micelles for curcumin solubilization and inhibition of cancer cell growth. *Eur. J. Pharm. Biopharm.* **2015**, *94*, 501−512.

(18) Gelderblom, H.; Verweij, J.; Nooter, K.; Sparreboom, A. Cremophor EL: The drawbacks and advantages of vehicle selection for drug formulation. *Eur. J. Cancer* **2001**, *37*, 1590−1598.

(19) Dhimitruka, I.; SantaLucia, J. Investigation of the Yamaguchi esterification mechanism. Synthesis of a Lux-S enzyme inhibitor using an improved esterification method. *Org. Lett.* **2006**, *8*, 47−50.

DOI: 10.1021/acs.oprd.9b00387
Org. Process Res. Dev. 2019, 23, 2707−2715

(20) Bagheri, M.; Bresseleers, J.; Varela-Moreira, A.; Meeuwissen, S. A.; Schiffelers, R. M.; Metselaar, J. M.; van Nostrum, C. F.; van Hest, J. C. M.; Hennink, W. E. effect of formulation and processing parameters on the size of mPEG-*b*-p(HPMA-Bz) polymeric micelles. *Langmuir* **2018**, *34*, 15495−15506.
(21) de Vos, R.; Goethals, E. J. End group analysis of commercial poly(ethylene glycol) monomethyl ether's. *Polym. Bull.* **1986**, *15*, 547−549.
(22) Talelli, M.; Rijcken, C. J. F.; Oliveira, S.; van der Meel, R.; van Bergen ene Henegouwen, P. M. P.; Lammers, T.; van Nostrum, C. F.; Storm, G.; Hennink, W. E. Reprint of 'nanobody - Shell functionalized thermosensitive core-crosslinked polymeric micelles for active drug targeting'. *J. Controlled Release* **2011**, *153*, 93−102.
(23) Kopeček, J.; Bažilová, H. Poly[N-(2-hydroxypropyl) methacrylamide]–I: radical polymerization and copolymerization. *Eur. Polym. J.* **1973**, *9*, 7−14.

DOI: 10.1021/acs.oprd.9b00387
Org. Process Res. Dev. 2019, 23, 2707−2715